Database for characterization of potential sites for CO2 storage in Northern Germany (https://doi.org/10.5880/GFZ.KHAG.2025.002)

Yifan Xu[a,b], Mrityunjay Singh[a], Cornelia Schmidt-Hattenberger[a], Márton Pál Farkas[a], Wolfgang Weinzierl[a], Tomas Fernandez-Steeger[b]

a. *Section 4.3 Geoenergy, GFZ Helmholtz Centre for Geosciences, Potsdam, Germany*
b. *Department of Engineering Geology, Technical University Berlin, 10587, Germany*

1. License

2. Citation

When using the data please cite:

Xu, Y.; Singh, M.; Schmidt-Hattenberger, C.; Farkas, M. P.; Weinzierl, W.; Fernandez-Steeger, T. (2025): Database for characterization of potential sites for CO2 storage in Northern Germany. GFZ Data Services. https://doi.org/10.5880/GFZ.KHAG.2025.002

The data are supplementary material to:

Xu, Y.; Singh, M.; Schmidt-Hattenberger, C.; Farkas, M. P.; Weinzierl, W.; Fernandez-Steeger, T. (2025): Developing a preliminary site selection method for direct air capture and CO2 storage technology with a case study in the North Germany. International Journal of Greenhouse Gas Control. 10.1016/j.ijggc.2025.104392

Table of Contents

3. Data description

The database help assess the technical feasibility questions for CO2 underground storage in North German Basin and the German North Sea region serving as a reference for “direct air capture and storage for reaching CO2 neutrality” project. The main purpose for this database was to gather uniform geological data information for characterizing depleted hydrocarbon fields and deep saline aquifers, supporting strategic decision making for pilot project to establish a direct air capture and storage demonstrator in Germany. All data collected for the database comes from public domains and therefore making it suitable for preliminary site screening and selection. However, detailed site characterization and further investigation are required for more comprehensive evaluation.

For each of the identified storage sites found from previous publication and projects (Höding et al., 2009; Hystories, 2022; Poulsen et al., 2013), nine parameters were selected for geological characterization for CO2 storage assessment, which are depth and thickness of storage formation, porosity and permeability, estimated storage capacity, caprock thickness, and reservoir integrity, as well as geothermal gradient. The determination of this parameters were generally following the instructions of International Organization for Standardization (2017), the ISO 27914:2017 standard outlines the requirements for carbon dioxide capture, transportation, and geological storage and other publications for site screening and selection instructions (Callas et al., 2022, 2023; Kim et al., 2022; Raza et al., 2016; Uliasz-Misiak et al., 2021), and further carved considering sound scientific approaches, best practice methodologies, availability of high-quality data, and in-situ storage conditions.

The geological coordinates have been converted to WGS 84 / UTM zone 33N with QGIS authority projection number as European Petroleum Survey Group (32633). Most geological parameters were extracted based on TUNB model (BGR, LAGB, LBEG, LBGR, LLUR, & LUNG, 2022), additional petrophysical information were mainly collected from Müller & Reinhold, (2011), Reinhold et al., (2011) and Petroleum Geological Atlas of the Southern Permian Basin Area, (2010) projects. Additionally, this database can also serve as a valuable resource for other types of underground storage characterization.

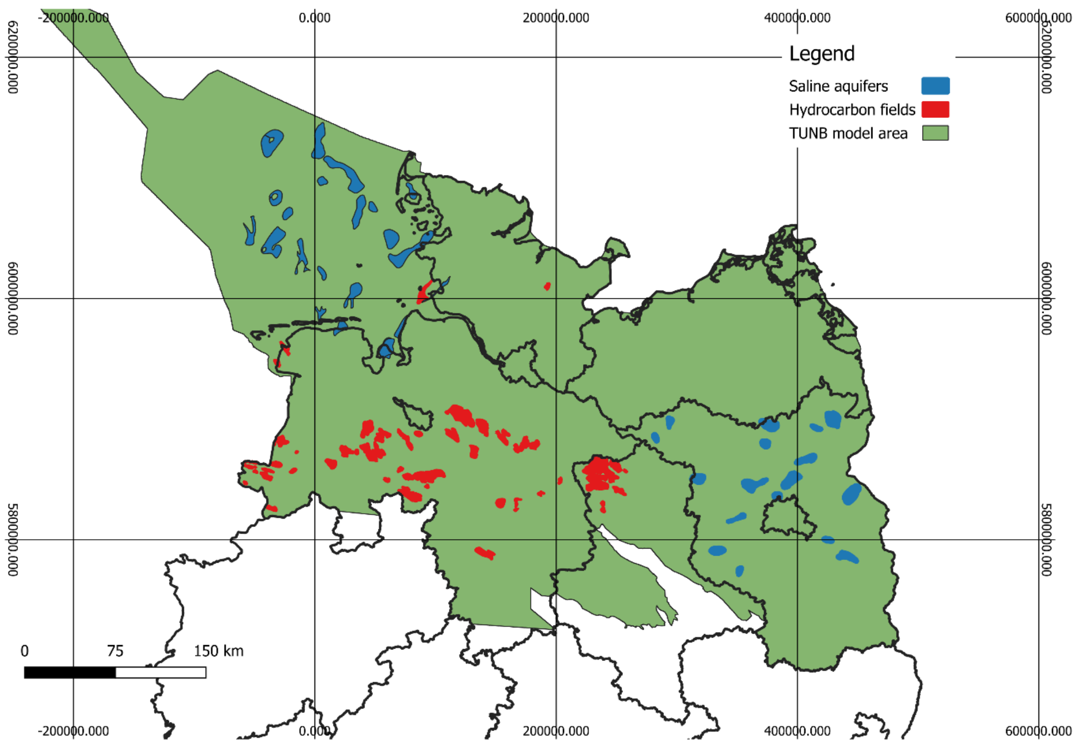

Figure 1: Identified CO_2 storage traps in our study region. Blue refers to deep saline aquifers and red refers to depleted oil and gas fields.

4. Data processing

4.1. Depth, thickness, faults information

Depth, thickness, fault structures are extracted using pvpython, which is a python-based interface that comes with ParaView, allowing users to automate data processing, visualization tasks, and create custom workflow. The pseudocode shown in *Table 1* shows the process for extracting depth, thickness and faults information for a storage trap, then loop it over to all traps in the study region. For depth and thickness, due to the heterogeneity at each storage site, we extracted the minimum, mean and maximum value in our data table, an example for how it looks like in the database was illustrated in *Figure 2*. The data extracted from TUNB model are presented in VTK file format (interfaces), therefore the algorithm is needed to convert interfaces data to raster data at each trap.

	A	B	C	G	H	I
1	OBJECTID	TRAP_ID	TRAP_NAME	GROSS_THICK_MIN_RES	GROSS_THICK_MEAN_RES	GROSS_THICK_MAX_RES
2	1060	DE_T_20120927105504191	Zechstein Daughter Unit 7	2.0	47.7777777777778	200
3	1061	DE_T_20120927105623346	Zechstein Daughter Unit 8	2.0	47.7777777777778	200
4	1062	DE_T_20120927110831538	Zechstein Daughter Unit 9	2.0	47.7777777777778	200
5	1109	DE_T_20120926162141938	Middle Buntsandstein Daughter Unit 16	10.0	92.5555555555556	400
6	1110	DE_T_20120926162329514	Middle Buntsandstein Daughter Unit 17	10.0	92.5555555555556	400
7	1111	DE_T_20120926162624125	Middle Buntsandstein Daughter Unit 18	10.0	92.5555555555556	400
8	1112	DE_T_20120926162956925	Middle Buntsandstein Daughter Unit 19	10.0	92.5555555555556	400
9	1113	DE_T_20120926164007868	Keuper Daughter Unit 1	2.0	78.0	400
10	1114	DE_T_20120926164339357	Keuper Daughter Unit 2	2.0	78.0	400
11	1115	DE_T_20120926164540569	Keuper Daughter Unit 3	2.0	78.0	400
12	1116	DE_T_20120926165126109	Middle Jurassic Daughter Unit 1	0.32	45.1952941176471	120
13	1117	DE_T_20120926165330939	Middle Jurassic Daughter Unit 2	0.32	45.1952941176471	120
14	1118	DE_T_20120926170030633	Middle Jurassic Daughter Unit 3	0.32	45.1952941176471	120
15	1119	DE_T_20120927082910801	Upper Rotliegend Daughter Unit 1	10.0	122.0	600
16	1120	DE_T_20120927083918962	Upper Rotliegend Daughter Unit 2	10.0	122.0	600
17	1063	DE_T_20120927111017883	Zechstein Daughter Unit 10	2.0	47.7777777777778	200
18	1064	DE_T_20120927111546992	Zechstein Daughter Unit 11	2.0	47.7777777777778	200
19	1065	DE_T_20120927111800184	Zechstein Daughter Unit 12	2.0	47.7777777777778	200
20	1066	DE_T_20120927112013657	Zechstein Daughter Unit 13	2.0	47.7777777777778	200
21	1067	DE_T_20120927112602239	Zechstein Daughter Unit 14	2.0	47.7777777777778	200
22	1068	DE_T_20120927113043039	Zechstein Daughter Unit 15	2.0	47.7777777777778	200
23	1069	DE_T_20120927113332938	Zechstein Daughter Uni 16	2.0	47.7777777777778	200
24	1121	DE_T_20120927084925833	Upper Rotliegend Daughter Unit 3	10.0	122.0	600
25	1122	DE_T_20120927085438160	Upper Rotliegend Daughter Unit 4	10.0	122.0	600
26	1123	DE_T_20120927085624989	Upper Rotliegend Daughter Unit 5	10.0	122.0	600
27	1124	DE_T_20120927085944716	Upper Rotliegend Daughter Unit 6	10.0	122.0	600
28	1125	DE_T_20120927090349215	Upper Rotliegend Daughter Unit 7	10.0	122.0	600
29	1126	DE_T_20120927090641267	Upper Rotliegend Daughter Unit 8	10.0	122.0	600
30	1070	DE_T_20120927115210968	Zechstein Daughter Unit 17	2.0	47.7777777777778	200
31	1071	DE_T_20120927115441866	Zechstein Daughter Unit 18	2.0	47.7777777777778	200
32	1072	DE_T_20120927135834236	Zechstein Daughter Unit 19	2.0	47.7777777777778	200

Figure 2: *Excerpt from the depth information stored in data table for different traps (completed data table is stored in zipfile as excel file.)*

4.1. Storage structure type

The storage structure information was interpreted based on depth spatial distribution within each storage traps. Detailed pseudo code for achieving this was displayed in Table 2. For each storage traps, the top and bottom trap depth distribution were extracted for all 91 traps and stored under zipfile, an example on how we classify different geological structures in this study were illustrated in table. An anticline is characterized by a shallower depth in the middle and deeper areas along the surrounding edges. Graben was interpreted as shallower at one side which usually bordered by normal faults as an impermeable layer. and deeper at the other side, while syncline was the opposite structure feature of an anticline, see Table 3.

Table 1: Pseudo code for extracting depth, thickness, faults information from VTK structure clipping within the geological boundary of the storage traps provided by shapefile.

Algorithm	`dgalShapeProcessing`
Input	`SavedBlocks`: Current number of saved blocks `shapefile`: path to the shapefile to process. `vtkGridFile`: path to the VTK grid file. `outfile`: File to store the output data. `append`: Boolean indicating if data should be appended or a new file should be created.
Output	Returns updated number of saved blocks after processing.
Steps:	
Read the VTK file	Use `LegacyVTKReader` to load `vtkGridFile`. Extract the bounds `vtkBounds` and update the pipeline.
Read the shapefile	Use `vtkGDALVectorReader` to load shapefile. Get number of blocks in shapefile (`numBlocks`).
Loop through each block in the shapefile	If block type is `vtkPolyData`: Extract the bounding box dimensions (xmin, xmax, ymin, ymax, zmin, zmax). Fetch the shape ID from the 'TRAP_ID' attribute.
Clip the VTK surface	Create a new clip using the shape's bounding box. Fetch and wrap the clipped VTK data.
Check the clipped points	If the clipped points (coords) are not empty: If `append` == `True`: Increate trap counter `t`. Append the clipped points and trap information to the output file. else Create a new output file and write the clipped points.
Update savedBlocks	Increment `savedBlocks` by 1.
Return	`savedBlocks`

Table 2: TUNB VTK Gridding of interfaces in trap shapes

Algorithm	**interfaces2raster**	
Input	single_SHP: Shapefile data for single polygon or multipolygon name_mapping_dict: spatial structure information from TUNB	
Output	xx, yy, mask_out, arr_Interfaces for the rasterized interfaces	
Steps:		
Initialize unit_name	Loop through name_mapping_dict.	
	If	single_SHP['TRAP_NAME'] starts with any value from the dictionary, set unit_name.
Create a raster grid		Get bounds (xmin, ymin, xmax, ymax) from single_SHP['geometry'].bounds Define a 100x100 grid of points (nx = 100, ny = 100). Generate xx and yy meshgrid arrays.
Convert shapefile geometry to matplotlib polygon		Initialize an empty list mpl_polygons. If shape == Polygon or Multipolygon: Extract exterior coordinates of the polygon and append them to mpl_polygons. Else print "Not supported polygon type".
Generate a mask for the raster grid points		For each polygon, determine which grid points fall inside the polygon. Create a mask (mask_out) indicating points within the shape.
Prepare an empty array for interface depths		Create a 3D array (arr_Interfaces) to store depth values for each interface (filled initially with NaN)
Interpolate interface data	For	each interface ("Top reservoir" and "Base reservoir"): Load depth data Perform linear interpolation to estimate depth values for the grid points. Apply the mask so only points inside the shape retain valid values. Store the interpolated depths in arr_Interfaces.
Plot the results	Create a plot for each interface showing the depth values within the shape.	
Return the results	Return the grid coordinates, the mask, and the interpolated interface depths	

__Table 3__: Trap structure example (complete structure figures are stored in zipfile)

Classification of trap structure	Trap example
Anticline	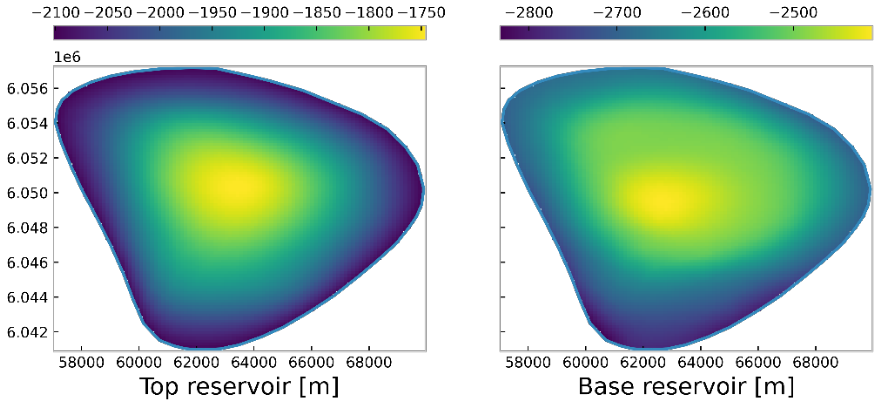
Graben	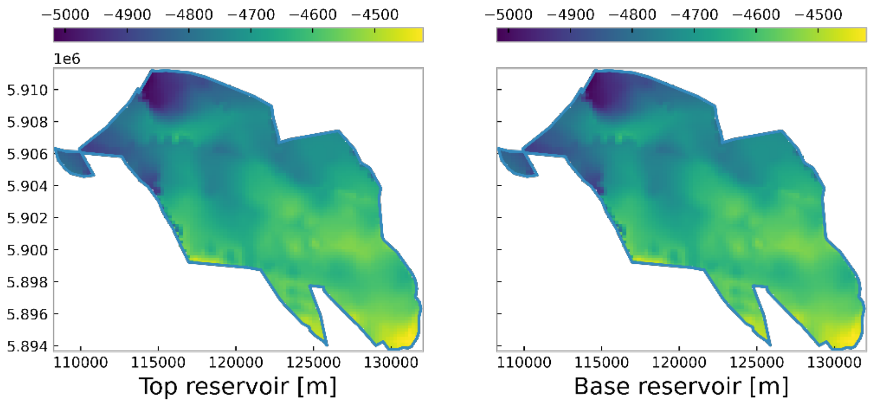
Syncline	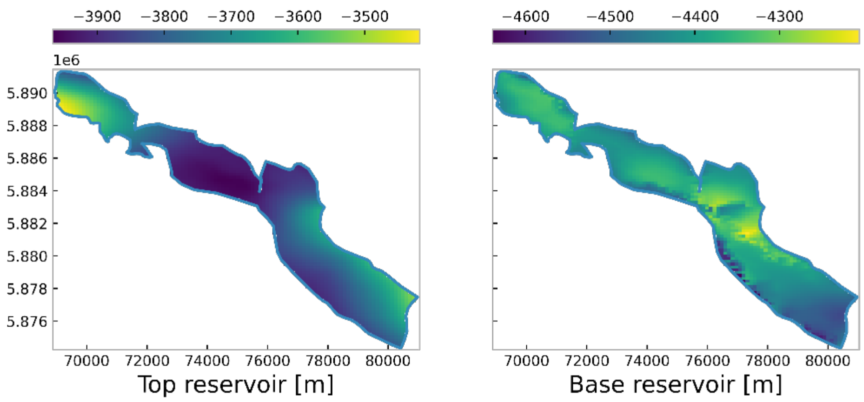

4.2. Porosity, permeability, thickness of traps.

The porosity, permeability and thickness information were collected as point data and rearrange into sequence from smallest to biggest value, then minimum, mean (median for permeability) and maximum value were extracted for each of this petrophysical parameters and assigned for each trap with the same storage formation, the idea is similar as what has been illustrated in 3.1.1. See detailed pseudo code in *Table 4*, with an illustration example of output figure plotting in *Figure 3*. The petrophysical data information was also storage in data table as delimited text file, an excerpt is shown in *Figure 4*.

Table 4: Pseudo code for generating petrophysical properties for traps in our study region.

Algorithm	`trap_petrophysical_info`
Input	`speicherkataster_dict`: dictionary for all storage formations identified in all traps with collected petrophysical data information. `dict_property`: dictionary for min, mean, max information for each storage formation.
Output	Plot for parameter values (porosity, permeability, and thickness)
Steps	
Load data	Load data for all properties
Loop through storage unit data	For each formation in `speicherkataster_dict:` Sort data for each property Store min, mean(median), max values in dictionary (`dict_property`)
Plot the figure for each property	Plot the cumulative distribution function and range using step and rectangle. Annotate the mean value on the plot.

	A	B	C	Q	R	S
1	OBJECTID	TRAP_ID	TRAP_NAME	POROSITY_MIN	POROSITY_MEAN	POROSITY_MAX
2	1060	DE_T_20120927105504191	Zechstein Daughter Unit 7	0.02	145	0.32
3	1061	DE_T_20120927105623346	Zechstein Daughter Unit 8	0.02	145	0.32
4	1062	DE_T_20120927110831538	Zechstein Daughter Unit 9	0.02	145	0.32
5	1109	DE_T_20120926162141938	Middle Buntsandstein Daughter Unit 16	0.12	0.210769230769231	0.3
6	1110	DE_T_20120926162329514	Middle Buntsandstein Daughter Unit 17	0.12	0.210769230769231	0.3
7	1111	DE_T_20120926162624125	Middle Buntsandstein Daughter Unit 18	0.12	0.210769230769231	0.3
8	1112	DE_T_20120926162956925	Middle Buntsandstein Daughter Unit 19	0.12	0.210769230769231	0.3
9	1113	DE_T_20120926164007868	Keuper Daughter Unit 1	0.09	0.201363636363636	0.3
10	1114	DE_T_20120926164339357	Keuper Daughter Unit 2	0.09	0.201363636363636	0.3
11	1115	DE_T_20120926164540569	Keuper Daughter Unit 3	0.09	0.201363636363636	0.3
12	1116	DE_T_20120926165126109	Middle Jurassic Daughter Unit 1	0.04	0.2335	0.45
13	1117	DE_T_20120926165330939	Middle Jurassic Daughter Unit 2	0.04	0.2335	0.45
14	1118	DE_T_20120926170030633	Middle Jurassic Daughter Unit 3	0.04	0.2335	0.45
15	1119	DE_T_20120927082910801	Upper Rotliegend Daughter Unit 1	0.02	0.101428571428571	0.15
16	1120	DE_T_20120927083918962	Upper Rotliegend Daughter Unit 2	0.02	0.101428571428571	0.15
17	1063	DE_T_20120927111017883	Zechstein Daughter Unit 10	0.02	145	0.32
18	1064	DE_T_20120927111546992	Zechstein Daughter Unit 11	0.02	145	0.32
19	1065	DE_T_20120927111800184	Zechstein Daughter Unit 12	0.02	145	0.32
20	1066	DE_T_20120927112013657	Zechstein Daughter Unit 13	0.02	145	0.32
21	1067	DE_T_20120927112602239	Zechstein Daughter Unit 14	0.02	145	0.32
22	1068	DE_T_20120927113043039	Zechstein Daughter Unit 15	0.02	145	0.32
23	1069	DE_T_20120927113332938	Zechstein Daughter Uni 16	0.02	145	0.32
24	1121	DE_T_20120927084925833	Upper Rotliegend Daughter Unit 3	0.02	0.101428571428571	0.15
25	1122	DE_T_20120927085438160	Upper Rotliegend Daughter Unit 4	0.02	0.101428571428571	0.15
26	1123	DE_T_20120927085624989	Upper Rotliegend Daughter Unit 5	0.02	0.101428571428571	0.15
27	1124	DE_T_20120927085944716	Upper Rotliegend Daughter Unit 6	0.02	0.101428571428571	0.15
28	1125	DE_T_20120927090349215	Upper Rotliegend Daughter Unit 7	0.02	0.101428571428571	0.15
29	1126	DE_T_20120927090641267	Upper Rotliegend Daughter Unit 8	0.02	0.101428571428571	0.15
30	1070	DE_T_20120927115210968	Zechstein Daughter Unit 17	0.02	145	0.32
31	1071	DE_T_20120927115441866	Zechstein Daughter Unit 18	0.02	145	0.32
32	1072	DE_T_20120927135834236	Zechstein Daughter Unit 19	0.02	145	0.32
33	1073	DE_T_20120927141507759	Zechstein Daughter Unit 20	0.02	145	0.32
34	1074	DE_T_20120927141834693	Zechstein Daughter Unit 21	0.02	145	0.32
35	1075	DE_T_20120927143226017	Middle Buntsandstein Daughter Unit 1	0.12	0.210769230769231	0.3
36	1127	DE_T_20120927091010057	Upper Rotliegend Daughter Unit 9	0.02	0.101428571428571	0.15
37	1128	DE_T_20120927100949297	Upper Rotliegend Daughter Unit 10	0.02	0.101428571428571	0.15
38	1076	DE_T_20120927143449021	Middle Buntsandstein Daughter Unit 2	0.12	0.210769230769231	0.3

***Figure 3:** Excerpt for petrophysical information in data table for different traps.*

5. File description

5.1. Description of data tables

The short name of the columns in the geological underground storage sites database and their description are provided in Table 5.

Table 5: *geological parameter data base for identified 92 traps in our study region (see full table under 2025-002_Xu-et-al_NGB.csv in zipfile).*

Column head	unit	Short description
OBJECTID	[-]	A unique identifier for each trap
TRAP_ID	[-]	A unique identifier for each trap
TRAP_NAME	[-]	The name of the geological trap
STRUCTURE	[-]	The type of the geological structure (e.g., graben, anticline)
STORAGE_CAPACITY_MEAN	[Mt]	The mean estimated storage capacity of the trap, calculated in million ton
STORAGE_CAPACITY_MAX	[Mt]	The mean estimated storage capacity of the trap, calculated in million ton
ASSESS_UNIT	[-]	The assessment unit, whether the trap is a hydrocarbon or aquifer trap unit
GROSS_THICK_MIN_RES	[m]	Minimum gross thickness of the trap, in meters (m)
GROSS_THICK_MEAN_RES	[m]	Mean gross thickness of the trap, in meters (m)
GROSS_THICK_MAX_RES	[m]	Maximum gross thickness of the trap, in meters (m)
DEPTH_MIN_RES	[m]	Minimum depth of the trap, in meters (m)
DEPTH_MEAN_RES	[m]	Mean depth of the trap, in meters (m)
DEPTH_MAX_RES	[m]	Maximum depth of the trap, in meters (m)
TEMP_GRADIENT	[°C/km]	Temperature gradient of the trap, measured in degrees Celsius per kilometer (°C/km)
PERM_MIN	[mD]	Minimum permeability of the reservoir, measured in millidarcies (mD)
PERM_MEDIA	[mD]	Median permeability of the reservoir, measured in millidarcies (mD)
PERM_MAX	[mD]	Maximum permeability of the reservoir, measured in millidarcies (mD)
POROSITY_MIN	[%]	Minimum porosity of the reservoir, given as a percentage (%)
POROSITY_MEAN	[%]	Mean porosity of the reservoir, given as a percentage (%)
POROSITY_MAX	[%]	Maximum porosity of the reservoir, given as a percentage (%)
FIELD_EXTET_MEAN	[m^2]	The average field extent, calculated in square meters
MIN_SEAL_THICK	[m]	Minimum thickness of the sealing layer above the trap, in meters
FAULT	[-]	The faults within the trap area
BUNDESLAND	[-]	The state or federal region where the trap is located (e.g., NI = Niedersachsen)
TEMP_EARTH	[°C]	Earth temperature of the reservoir, in degrees Celsius (°C)
TEMP_MEAN	[°C]	Mean temperature of the reservoir, in degrees Celsius (°C)
RHO_CO2	[kg/m^3]	The density of CO_2 in kilograms per cubic meter (kg/m^3), relevant for CO_2 storage calculations.
geometry	[-]	Geometric information of the trap (e.g., polygons representing the location of the trap in a geospatial format)
Projection_Info	[-]	Information about the coordinate reference system used (e.g., EPSG:32633)
X, Y	[-]	The coordinates of the trap, based on the projection system
SCORE_MEAN	[-]	Mean scores for the storage potential and suitability, based on various geological and operational factors in this study.
SCOREW_MEAN	[-]	Weighted mean scores for the storage potential and suitability, based on various geological and operational factors in this study.
SCORE_MAX	[-]	Max scores for the storage potential and suitability, based on various geological and operational factors in this study.
SCOREW_MAX	[-]	Weighted max scores for the storage potential and suitability, based on various geological and operational factors in this study.

6. References

BGR, LAGB, LBEG, LBGR, LLUR, LUNG. (2022). 3D-Modell des geologischen Untergrundes des Norddeutschen Beckens (Projekt TUNB). Erstveröffentlichung 2021, Version 2022. Retrieved from https://gst.bgr.de

Callas, C., Kovscek, A. R., & Benson, S. M. (2023, April). Incorporating Data Confidence and Scoring Sensitivity into Site Selection Ranking in Depleted Hydrocarbon Reservoirs. In Offshore Technology Conference (p. D011S010R006). OTC. Retrieved from: https://sccs.stanford.edu/sites/g/files/sbiybj17761/files/media/file/otc-32331-ms_0.pdf

Callas, C., Saltzer, S. D., Davis, J. S., Hashemi, S. S., Kovscek, A. R., Okoroafor, E. R., ... & Benson, S. M. (2022). Criteria and workflow for selecting depleted hydrocarbon reservoirs for carbon storage. Applied Energy, 324, 119668, https://doi.org/10.1016/j.apenergy.2022.119668

Höding, T., Göthel, M., & Stackebrandt, W. (2009). Geologische Möglichkeiten für die CO2-Speicherung in Brandenburg. Brandenburg. Geowiss. Beitr, 16(1/2), 1-18. Retrieved from: https://lbgr.brandenburg.de/sixcms/media.php/9/BGB-1-2_09_Hoeding_1-18.pdf

Hystories. (2022). Hydrogen Storage in European Subsurface (Hystories) project: 3D model and storage data viewer. https://www.arcgis.com/apps/dashboards/630ec7b3cbd54e39b4111e397315ae99

ISO (International Organization for Standardization). (2017). ISO 27914:2017: Carbon dioxide capture, transportation and geological storage - Geological storage. ISO.

Kim, T. W., Callas, C., Saltzer, S. D., & Kovscek, A. R. (2022). Assessment of oil and gas fields in California as potential CO2 storage sites. International Journal of Greenhouse Gas Control, 114, 103579. https://doi.org/10.1016/j.ijggc.2022.103579

Müller, C., & Reinhold, K. (2011). Geologische Charakterisierung tiefliegender Speicher-und Barrierehorizonte in Deutschland-Speicher-Kataster Deutschland. Schweizerbart. https://doi.org/10.1127/sdgg/74/2011/9

Petroleum geological atlas of the Southern Permian Basin Area. (2010). [Map]. TNO Geological Survey of the Netherlands. Retrieved from https://www.nlog.nl/southern-permian-basin-atlas

Poulsen, N., Holloway, S., Kirk, K., Neele, F., & Smith, N. (2015). CO2StoP: A project mapping both reserves and resources for CO2 storage in Europe. Geological Survey of Denmark and Greenland Bulletin, 33, 85-88. https://setis.ec.europa.eu/european-co2-storage-database

Raza, A., Rezaee, R., Gholami, R., Bing, C. H., Nagarajan, R., & Hamid, M. A. (2016). A screening criterion for selection of suitable CO2 storage sites. Journal of Natural Gas Science and Engineering, 28, 317–327. https://doi.org/10.1016/j.jngse.2015.11.053

Reinhold, K., Müller, C., & Riesenberg, C. (2011). Informationssystem Speichergesteine für den Standort Deutschland-Synthese. Bundesanstalt für Geowissenschaften und Rohstoffe, Berlin/Hannover. Retrieved from: https://www.bgr.bund.de/DE/Themen/Nutzung_tieferer_Untergrund_CO2Speicherung/Projekte/CO2-Speicherung+Nutzungspotenziale/Abgeschlossen/speicherkataster.html

Uliasz-Misiak, B., Lewandowska-Śmierzchalska, J., & Matuła, R. (2021). Criteria for selecting sites for integrated CO2 storage and geothermal energy recovery. Journal of Cleaner Production, 285, 124822. https://doi.org/10.1016/j.jclepro.2020.124822